

# Lightweight, Conformal Antennas for Robotic Flapping Flyers

***Kamal Sarabandi<sup>1</sup>, Jungsuek Oh<sup>2</sup>, Leland Pierce<sup>1</sup>, Kunigal Shivakumar<sup>3</sup>,  
and Shivalingappa Lingaiah<sup>3</sup>***

<sup>1</sup>The Radiation Laboratory, Department of Electrical Engineering and Computer Science  
The University of Michigan  
Ann Arbor, MI 48109-2122 USA  
Tel: +1 (734) 764-0500; E-mail: sarabandi@umich.edu; lep@umich.edu

<sup>2</sup>Samsung Research America - Dallas  
1301 E Lookout Dr., Richardson, TX 75082 USA  
E-mail: jungsuek.oh@samsung.com

<sup>3</sup>Center for Composite Materials Research, Department of Mechanical Engineering  
North Carolina A&T State University  
Greensboro, NC 27411 USA  
Tel: +1 (336) 285-3203; E-mail: kunigal@ncat.edu; shivalingappal@yahoo.com

---

## Abstract

Using wings on small flying robots for embedded antennas can provide a flexible and lightweight solution for communications from these platforms. The fabrication of ultra-lightweight, high-strength polyimide nanopaper fabric from which the wing is built is outlined. Such materials can be used to build multilayer, lightweight electronics in a variety of other situations. After outlining the fabrication of the nanopaper, designs for two different antenna-embedding techniques are presented. First, a simple embedded wire antenna is fabricated and measured, followed by a more-complex printed antenna design. Each process is outlined and trade-offs are presented. Both designs worked well, and can be adapted for use in other similar scenarios.

Keywords: Antennas; mobile robots; flexible printed circuits; mobile communication

## 1. Introduction

**F**lying robots are becoming important for military and civilian uses [1, 2]. Due to the high energy cost of propulsion, making these platforms very lightweight is a key design goal. For palm-sized versions, flapping wings are one design feature that can trade off speed for enhanced endurance. A project funded by the Army aimed to design the next-generation reconnaissance robot that used flapping wings [3-5]. In order to provide reliable communications with such robots, careful design of embedded antennas was required.

This paper explores the idea of embedding antennas in the wings of such a robot. Using the wings provides two

main advantages over using the robot's body: (1) a large area to work with, which enables high-bandwidth antennas; and (2) separation from the other electronics of the platform, which can compromise the antenna's performance.

Flexible antennas have a wide spectrum of applications in wireless communication, where the antennas are integrated with conformal electronics platforms or objects [6-9]. Some of these applications involve using a paper substrate with human-wearable electronics as the main application area, which is quite different from the current application. Recently, a novel flexible antenna integrated with a flexible solar-cell array, suitable for use as a lightweight multifunctional wing of a flapping robot, was reported [10].

The wings, made of ultra-thin materials incorporating the embedded antenna, must be light and strong enough to provide lift during flapping without tearing. In one project dealing with insect flight [11], the wing loading was found to be of the order of  $1 \text{ N/m}^2$ . Other projects have used wings with embedded actuators [12, 13] to maximize lift and reduce drag. The antenna's structure must also provide minimal loading on the wings, in order to avoid degrading the efficiency of the flapping actuation. The super light weight and tensile characteristics of electro-spun Polyimide nanopaper are very promising for such stringent needs.

Hence, the wings used in this project were fabricated using a composite of extremely low-density – yet high strength – polyimide nanopaper fabric [14], plus a very thin layer of fiberglass. The remainder of this paper explains how the polyimide nanopaper was fabricated, and then the design, fabrication, and measurements for two different embedded antennas.

## 2. Nanopaper Wings

### 2.1 Background

Nanopaper is made using a technology similar to that used for making paper. The cellulose nanofibers used in making paper are 5 nm to 20 nm in diameter, and about  $5 \mu\text{m}$  in length, resulting in a large aspect ratio (about 250). When distributed in random orientations, these fibers offer isotropic properties, as well as superior tensile stiffness and strength. Nanopaper processes can be classified into two types: filtration of nanofiber suspensions followed by air drying [15, 16], and hot pressing [17-19] of the wet gel. The fibers are held in place by capillary tension and/or hydrogen bonding. These nanopapers have been shown to have a combination of high elastic modulus, tensile strength, toughness, optical transparency, low thermal expansion, and excellent oxygen barrier properties.

Electro-spinning of polymer solutions enables the production of much longer fibers [20] by applying a high voltage between the nozzle and the drum [21, 22, 14]. This electric field guides and pulls the fiber between the drum and the nozzle. The properties of the nanofiber can be controlled by the choice of the polymer and the parameters of the electro-spinning process. Electro-spun fabric is obtained in layers of non-woven fibers, and its bulk tensile properties are poor. In [14], Lingaiah et al. showed how to fuse the nanofibers at crossover points to make strong nanopaper. This was demonstrated with Nylon-66 nanofibers, and later extended to polyimide nanopapers [23] for high-temperature applications.

Electro-spun polyimide nanopaper has a broad range of applications requiring super lightweight structural flexibility and tolerance, due to the increased demand for low-mass, low-power, and flexible electronic devices [24-26].

## 2.2 Fabrication

Fabrication of polyimide nanopaper involves three major steps: solution preparation, spinning, and fusing. The solution is prepared with 20% by weight polyimide, dissolved in 99% N,N-Dimethyl formamide (DMF). This solution is then squeezed through a syringe (with a needle diameter of 0.36 mm) to produce a thin fiber, as shown in Figure 1. There is a rotating cylinder on which the fibers are deposited. A 30,000-volt potential difference between the drum and the nozzle is used to pull the solution into a thin thread, with a diameter of between 280 nm and 510 nm. This thread is then wound onto the rotating drum. During this process, the syringe is moved slowly lengthwise along an axis parallel to the axis of the drum, back and forth, in order to uniformly coat the cylinder. After two hours, the density of fibers on the drum is about  $4.5 \text{ g/m}^2$ . At this stage, the nanofibers are loosely packed, and must be compacted and fused at crossover points to make nanopaper with the required stiffness and strength properties.

Fusing the nanopaper must be carefully done to avoid stress concentrations that will compromise the strength of the resulting paper. The paper is hence sealed in a vacuum bag, which is then evacuated to a pressure of 133 Pa, much less than atmospheric pressure. Heat is applied at a temperature just below the glass-transition temperature of the fibers, in this case,  $330^\circ \text{ C}$ . After three minutes, the nanofibers have softened and fused (see Figure 2).

The measured elastic modulus of the nanopaper was 1 GPa, with a strength of 65 MPa, which made it strong enough to be used for the wings in a robotic flapper. This material was also attractive for wings due to its low density ( $4.5 \text{ g/m}^2$ ) and hence low overall weight for large wings.

## 3. Wire Antenna

### 3.1 Design

To start, we decided to use the simplest antenna technology: a curved wire dipole. To accomplish this, we chose a conductive thread made from steel and nylon, as a first try at using a material that was both conductive and wear-resistant. The mechanical drawing (Figure 3) shows the required spiral shape that it was to have had when embedded in the fabric, to provide an antenna with a center frequency of 1.3 GHz.

### 3.2 Fabrication

To enhance the strength, it was initially decided to embed the antenna between multiple nanopaper layers. The following process was followed to embed the metallic thread in the nanopaper layers (see Figure 4):

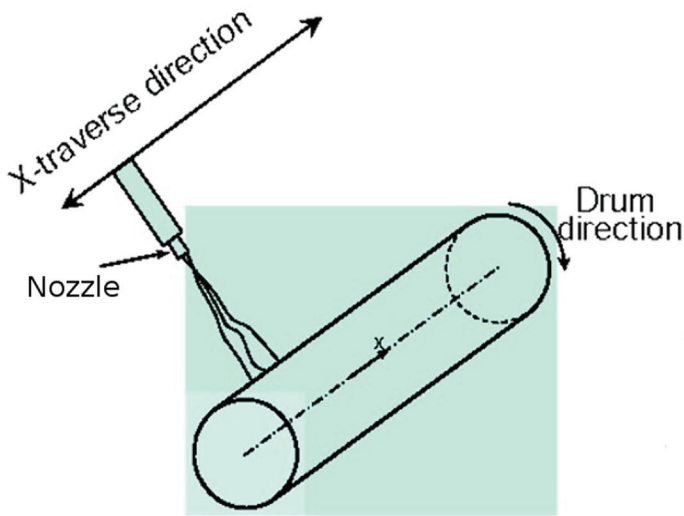


Figure 1a. A diagram of the major aspects of the X-traverse electro-spinning setup.

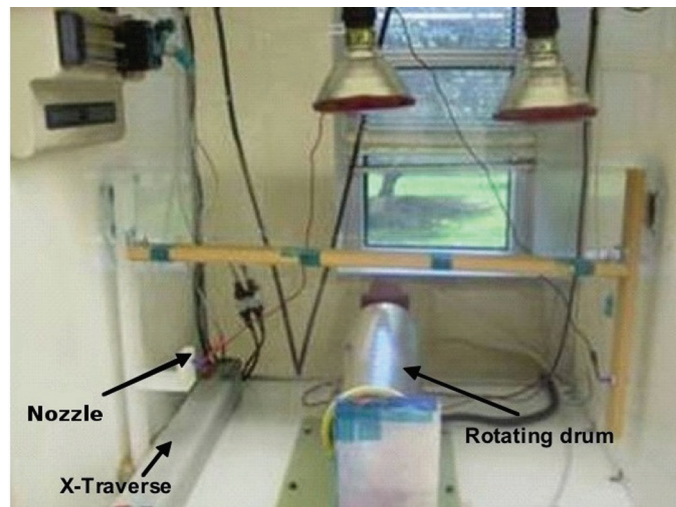


Figure 1b. A photo of the actual X-traverse electro-spinning setup.

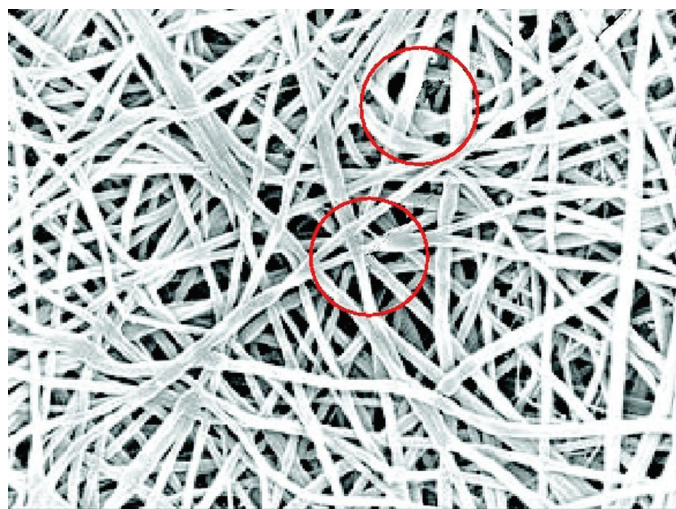


Figure 2. The thermal fusing of nanopaper at crossover points. The fusing junctions are circled in red. The fiber diameters ranged from 45 nm to 160 nm.

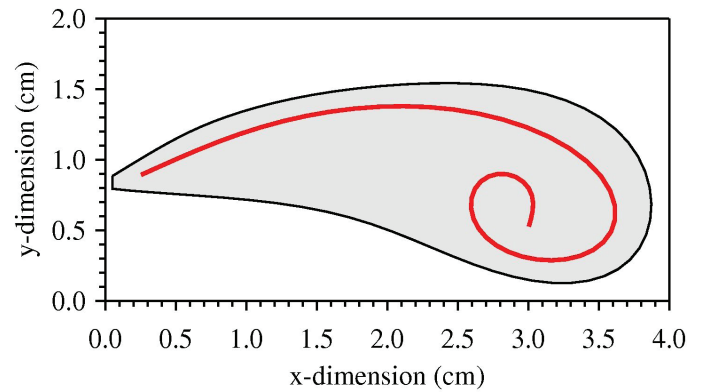


Figure 3. The schematic of the wire antenna as it would appear in a wing. The red line indicates the shape for the metal thread. The gray area is the intended wing shape.

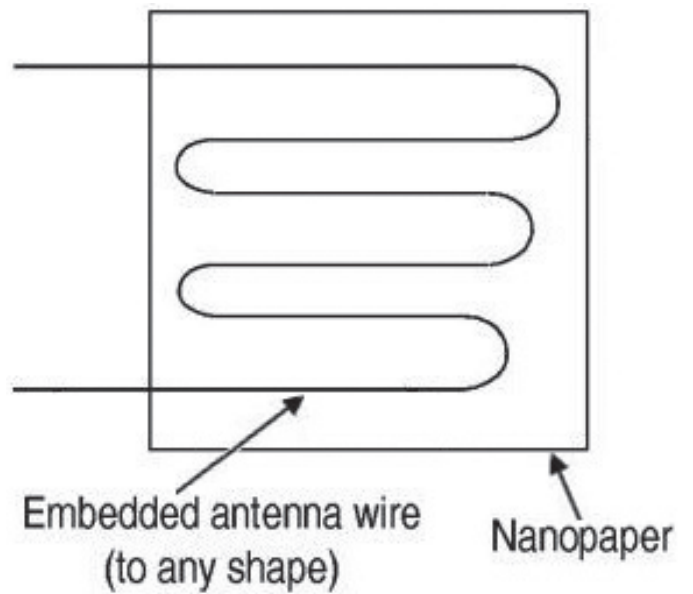


Figure 4a. The process for embedding the wire antenna between layers of nanopaper: a top view of a generic wire antenna as it would be embedded between paper layers.

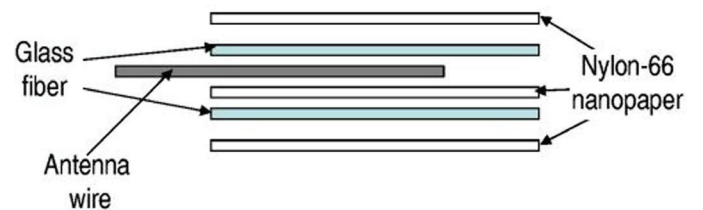
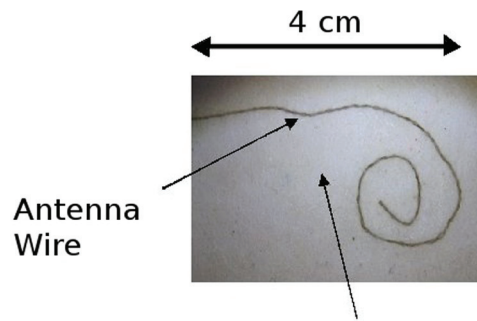


Figure 4b. A side view of the assembled layered structure, showing the Nylon-66 nanopaper, the glass-fiber reinforcement layers, and the antenna wire layer.

1. Each nanopaper layer was fabricated separately.
2. The antenna was formed to an approximate desired shape, and carefully aligned with the other paper layers.
3. The assembly was placed in a vacuum bag.
4. Once the bag was depressurized, it was then heated at 200° C for three minutes.
5. The wing with embedded antenna was then removed from the bag, with all layers bonded to each other.

The successfully embedded antenna/wing structure is shown in Figure 5, with the spiral antenna wire just visible through the translucent Nylon-66 paper layers.



**Nylon-66 glass fiber reinforced nanopaper**

**Figure 5. A top view photo of the wire antenna embedded in Nylon-66 electro-spun fabric reinforced with glass fibers. The light area is the paper, with a darker spiral pattern where the antenna wire shows through the translucent paper.**

### 3.3 Measurements

The structure of the nanopaper with the embedded antenna is very flexible and conformable, and so could not stand on its own. For measuring the antenna, we first attached it to a Styrofoam backing. We then placed the antenna and Styrofoam over a ground plane, to form a monopole antenna. This configuration was used in order to simulate the operational scenario where the flapping robot had two wings, each with an antenna, facing each other. The ground plane was used to form the image, which simulated the existence of the antenna in the “other” wing. This measurement setup is shown in Figure 6.

The antenna’s response was then measured using a vector network analyzer to determine the operating frequency. The result of the  $S_{11}$  measurement is shown in Figure 7. The measured antenna frequency response showed a very good impedance match at the desired frequency of 1.3 GHz. Also shown is the harmonic response at 2.6 GHz.

### 3.4 Lessons

The remarkably straightforward process for embedding the wire antenna in the nanopaper/fiberglass composite structure was easy and worked well. However, the antenna wire did not easily hold its shape during the process, and so the resulting antenna frequency could not be easily set. Future antennas of this type will require a jig or similar device for accurately forming the wire antenna’s shape before starting the embedding process. The multi-layer approach used here with nanopaper and fiberglass sheets also unnecessarily increased the wing’s mass. As an alternative, a more-accurate fabrication process was considered next. In this process, we explored the idea of using lithography to print the antenna directly on the nanopaper. This is discussed in the following section.

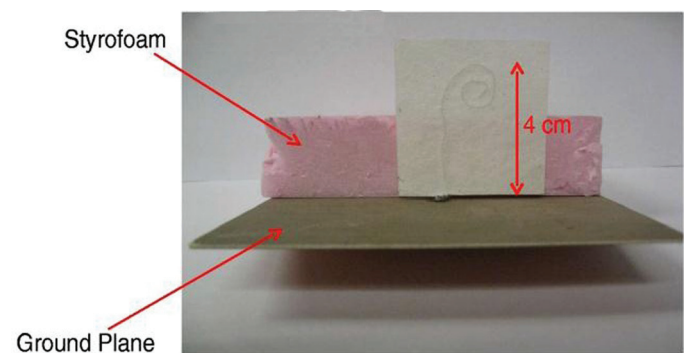


**Figure 6. The wire antenna is shown mounted vertically with a Styrofoam backer, placed on top of the copper ground plane. The dimensions of the ground plane were 12 cm by 12 cm.**

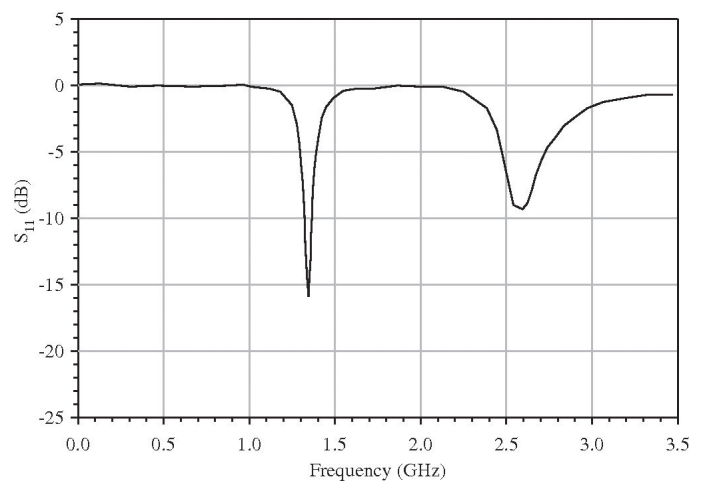


**Figure 7. The measured antenna frequency response, which showed a very good impedance match at the desired frequency of 1.3 GHz. Also shown is the harmonic response at 2.6 GHz.**

## 4. Printed Folded Dipole

This section presents the design, fabrication, and testing of a conformal UHF antenna on a single layer of nanopaper using a lithography method. Due to the limited size of the wing, an antenna operating at 400 MHz had to be confined to an area of 9 cm × 5.3 cm. To evaluate the performance of the proposed design, a monopole prototype over a ground plane was tested. The ground plane was used to simulate the symmetric geometry when two wings were used, forming a dipole antenna.

### 4.1 Design

The large size of conventional planar antennas conflicts with the limited space on the wing of the flapping robotic platforms. In this situation, a simple approach to antenna design can be the utilization of a quarter-wavelength monopole antenna. Bending the antenna appropriately to be fit in the wing can achieve the required resonant frequency. However, it was found that the bent-antenna topology aggravates the impedance matching to a 50-ohm feed. Figure 8 shows straight and bent quarter-wavelength monopole antennas (denoted by case a, and cases b and c, respectively). Comparison among the three cases showed the effects of the bent topology. The antennas were designed to operate at the same frequency of 390 MHz, and their input impedance ( $Z_{11}$ ) and radiation patterns were simulated using Ansoft *HFSS 13.0*. Figure 9 shows the real and imaginary parts of the input impedance ( $Z_{11}$ ) of the antennas corresponding to cases a, b, and c. The change in the real part of the impedance from 36 ohms to 9 ohms at the design frequency made impedance matching to a 50-ohm feed a challenge.

The decrease in the input impedance could be compensated for by considering a folded-antenna structure. This folding technique utilized the well-known fact that the input impedance of the  $\lambda/2$  folded dipole antenna is four times higher than that of the  $\lambda/2$  dipole antenna. Figure 10 shows the miniaturized folded monopole antenna, where one end of the antenna was shorted to ground. Tailoring the metallic trace fit into the wing's shape resulted in the design shown in Figure 10. Figure 11 shows the real and imaginary parts of the input impedance of the proposed antenna. As expected, the value of the real part at 390 MHz was increased to around 50 ohms, providing the capability of impedance matching to the 50-ohm feed. It was noted that this proposed antenna topology resulted in positioning a shunt-resonant frequency closer to the original series-resonant frequency. This caused the sharper slope of the  $Z_{11}$  of the proposed antenna around the series-resonant frequency. The impedance matching employing the proposed folded topology therefore came at the expense of decreased antenna bandwidth related to the slope of  $Z_{11}$ . Figure 12 shows the simulated  $S_{11}$  of the proposed antenna, and for cases a, b, and c. As discussed above, while the proposed antenna showed significant enhancement in impedance matching compared to cases b and c, the bandwidth of the proposed antenna was narrower than that of the straight quarter-wavelength monopole antenna (case a).

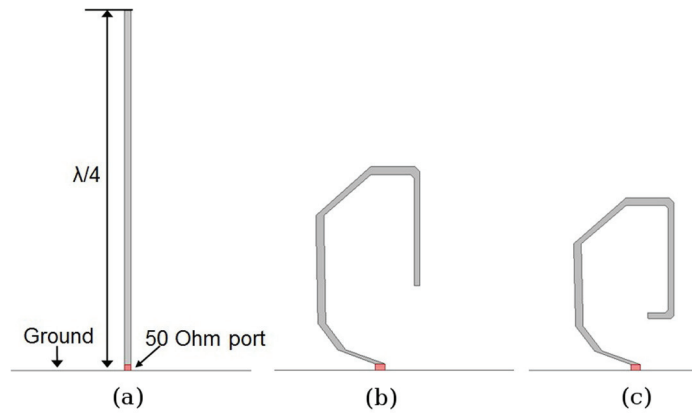


**Figure 8.** The design evolution of the printed antenna: (a) straight and (b, c) folded quarter-wavelength monopole antennas.

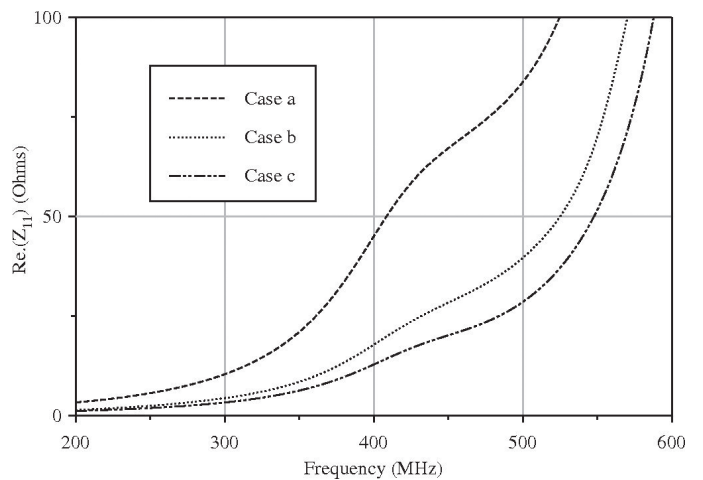


**Figure 9a.** The real part of the simulated input impedance of the antennas corresponding to designs a, b, and c in Figure 8.

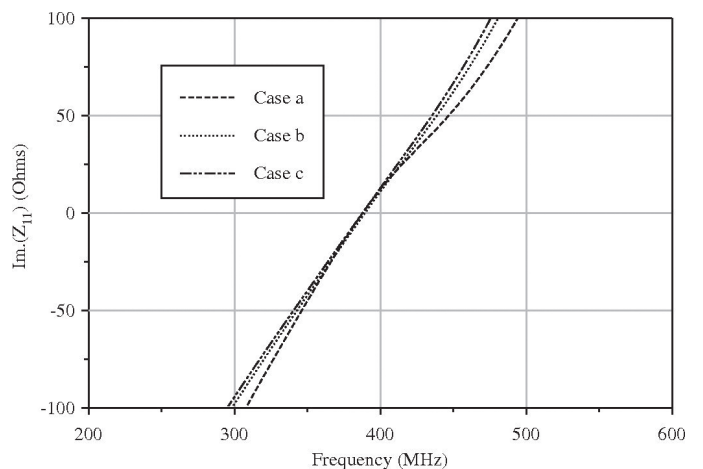


**Figure 9b.** The imaginary part of the simulated input impedance of the antennas corresponding to designs a, b, and c in Figure 8.

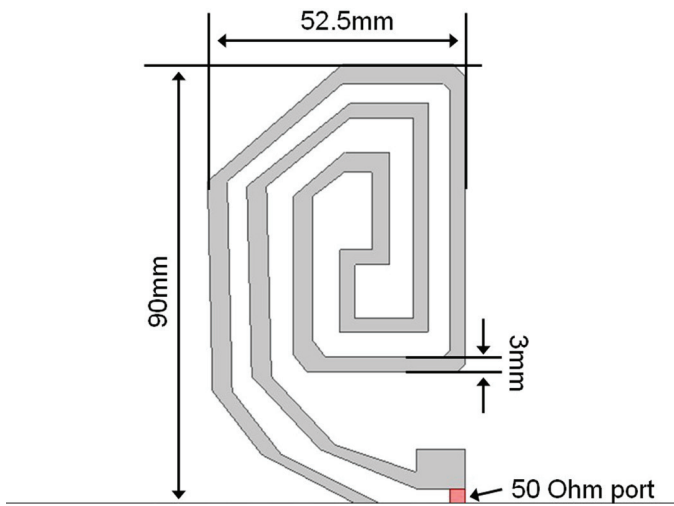


**Figure 10.** The topology of the proposed miniaturized folded monopole antenna.

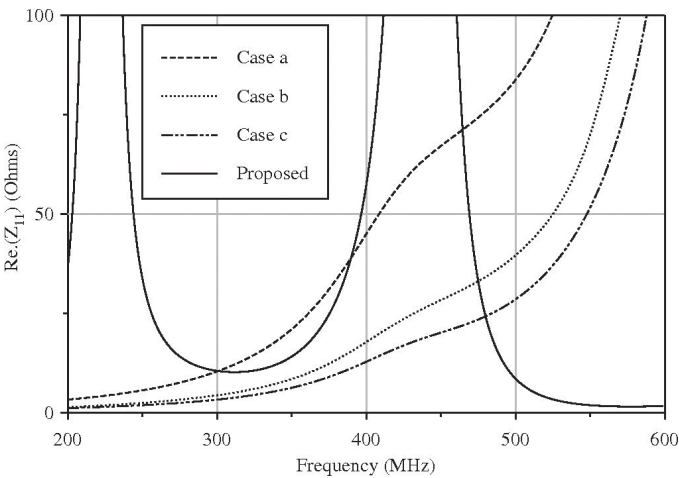


**Figure 11a.** The real part of the simulated input impedance of the proposed miniaturized folded monopole antenna in Figure 10.

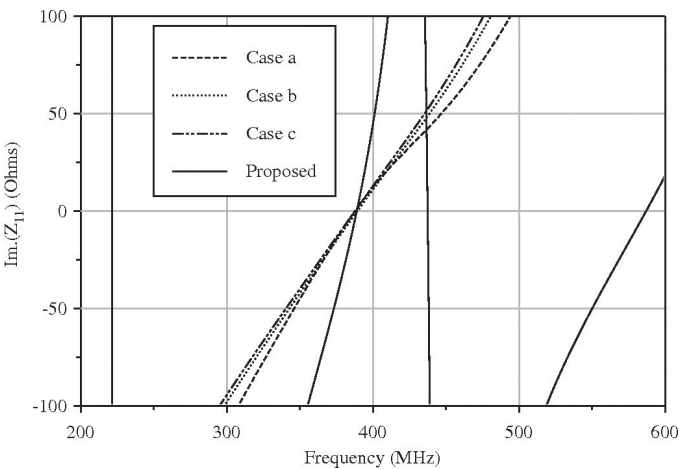


**Figure 11b.** The imaginary part of the simulated input impedance of the proposed miniaturized folded monopole antenna in Figure 10.

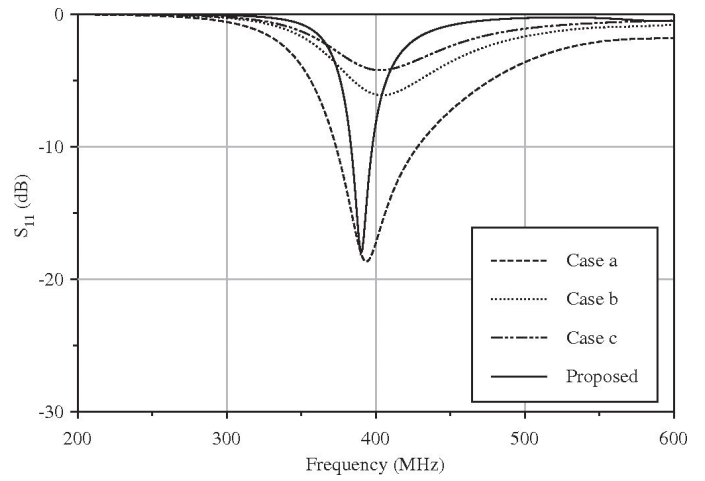


**Figure 12.** The simulated  $S_{11}$  of the proposed antenna compared with cases a, b, and c.

## 4.2 Fabrication

In order to deposit a metal layer for the antenna geometry on the nanopaper, three common fabrication methods (liftoff, etch-back and shadow mask) were considered. Figure 13 diagrams the three fabrication methods. In the liftoff method, photo-resist (PR) was first deposited on the nanopaper, and exposed to light with a proper mask. Photo-resist corresponding to the antenna pattern was then removed. This process was finished by depositing metal on the entire surface and then dissolving the rest of the photo-resist, which was covered with metal. The metal over photo-resist was also removed when the photo-resist was dissolved, and only the areas where there was no photo-resist would be covered by metal. Alternatively, in the etch-back method, a metal layer was first deposited on the nanopaper, and then the metal layer was covered by photo-resist. After exposure to light with a proper mask, photo-resist on the area not covering the antenna pattern was dissolved. Finally, the metal not covered by the remaining photo-resist was etched.

Applying the aforementioned two methods for the antenna on the nanopaper, two problems caused by the use of chemical solutions were found:

1. Once the nanofabric got wet with the solutions, the adhesion between the metal layer and nanofabric was lost.
2. During the chemical process, if the nanofabric was combined with liquid-type photo-resists, the photo-resists could not be completely removed with the developer.

Because of these problems, using a shadow mask which did not require the use of chemical solutions was the only practical method that could be used. Using a shadow mask and sputtering system, an aluminized UHF folded-monopole antenna could

be fabricated without damaging the nanopaper. We chose aluminum because of its high conductivity and low specific mass.

In order to obtain high-conductivity metal traces, the metal thickness should be about three times the skin depth. For aluminum at 390 MHz, this resulted in a required metal thickness of about 15  $\mu\text{m}$ . Figure 14a shows a photo of the fabricated antenna, mounted on a Styrofoam block. The final weight of the nanopaper and antenna was 0.18 g. We also performed a flexibility test on the fabricated antenna, repeatedly forming it around a circular curve with a half-inch radius of curvature (see Figure 14b). This was to simulate the effects due to flapping. No cracking of the metal traces was observed, nor was tearing of the paper. The measurements, presented next, were done after the flexibility tests, in order to show the expected performance after many flapping cycles.

### 4.3 Measurements

Figures 15 and 16 show the measured  $S_{11}$  and radiation patterns of the fabricated nanopaper antenna, compared to the

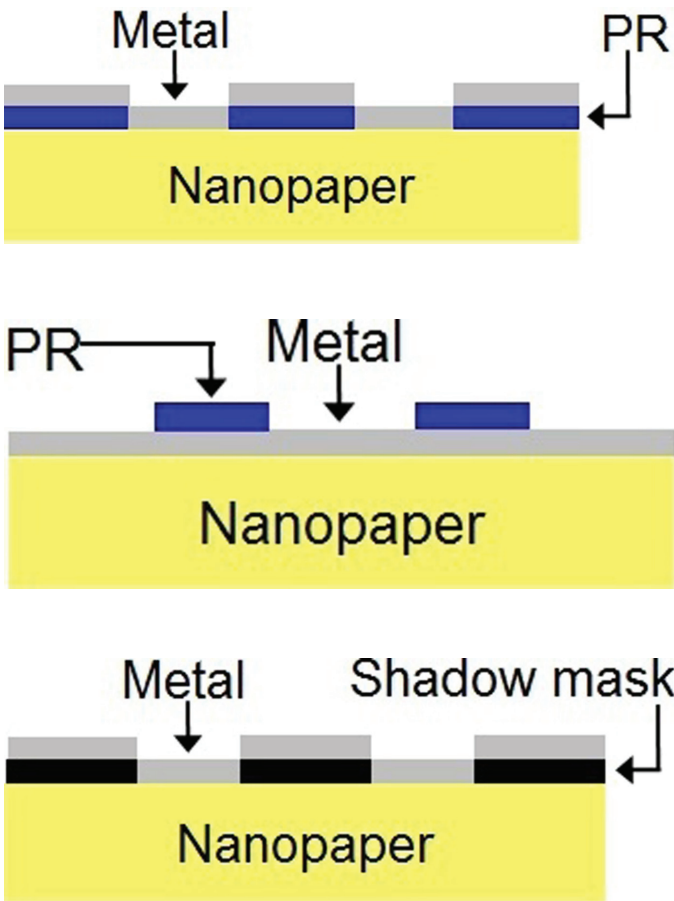


Figure 13. The fabrication of the printed antenna on the nanopaper substrate.

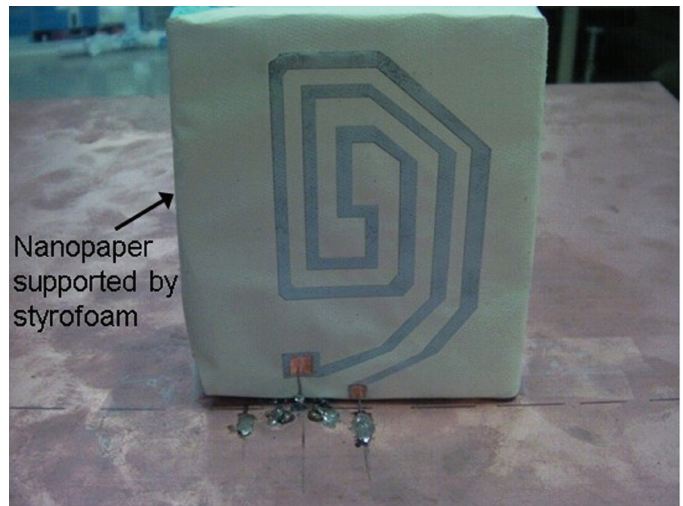


Figure 14a. The nanopaper antenna, supported by Styrofoam for measurements.



Figure 14b. A demonstration of the nanopaper antenna's flexibility.

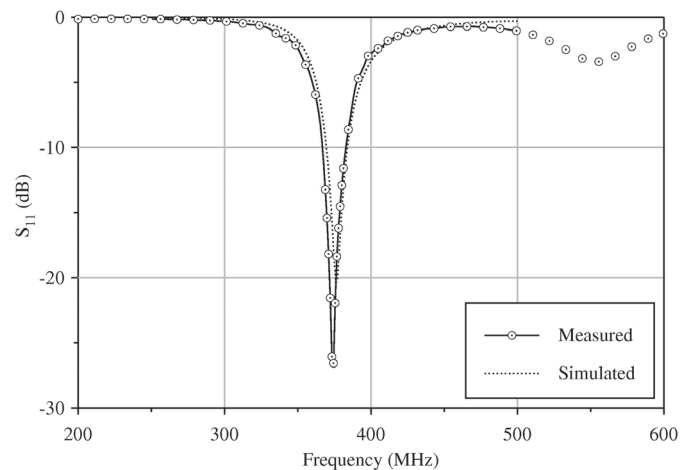
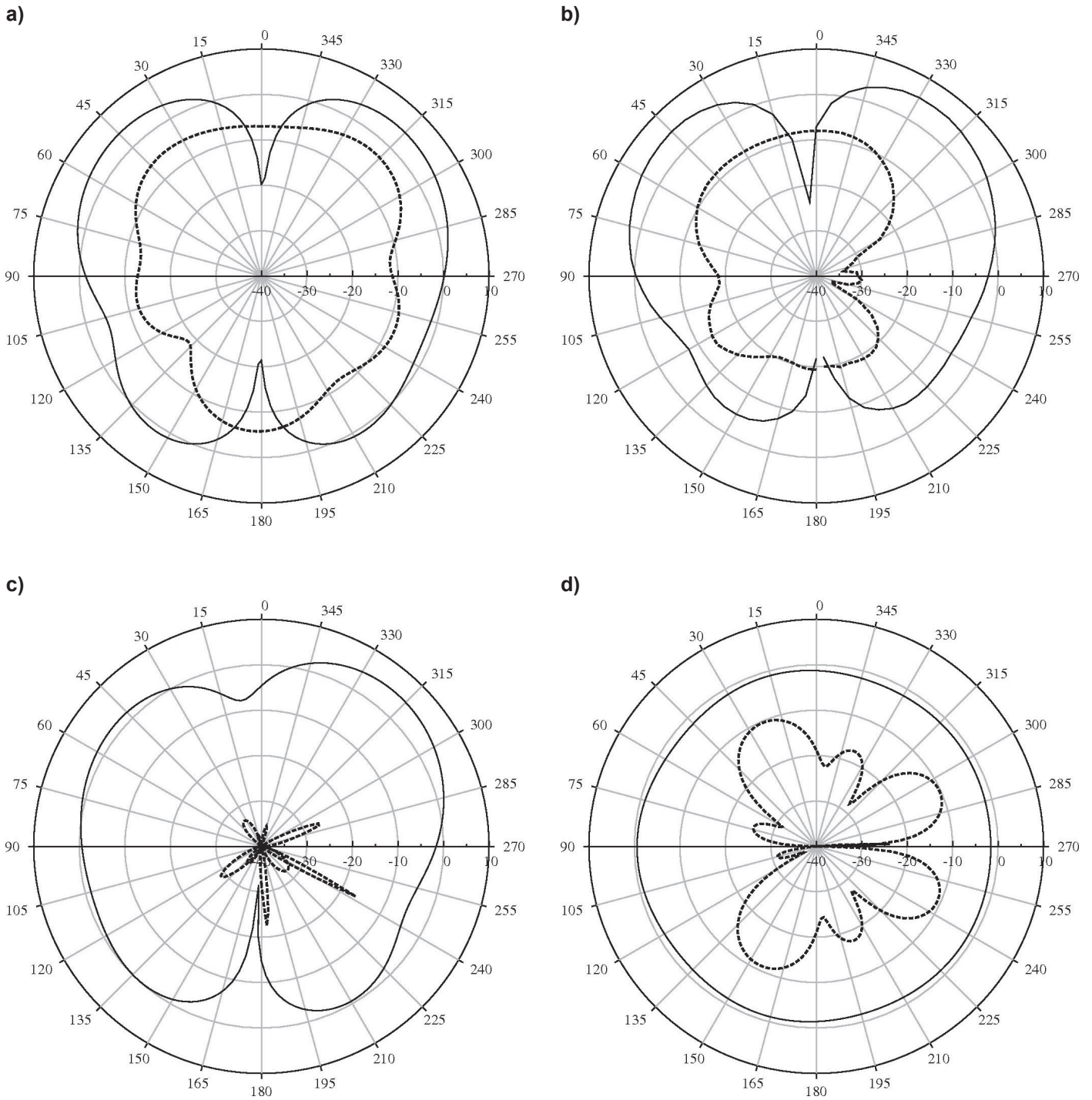
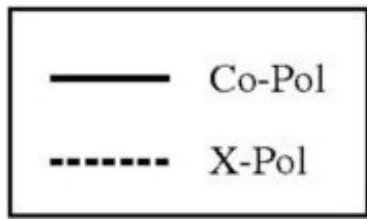


Figure 15. The measured  $S_{11}$  of the proposed antenna compared with the simulation.



**Figure 16. The radiation patterns of the proposed antenna: (a) the simulation on the  $yz$  plane, (b) the measured pattern on the  $yz$  plane, (c) the simulation on the  $xz$  plane, and (d) the simulation on the  $xy$  plane.**



simulated results. For measuring the antenna, we first attached it to a Styrofoam backing, and then placed the antenna and Styrofoam over a large ground plane, to form a monopole antenna. This configuration was used in order to simulate the operational scenario where the flapping robot had two wings, each with an antenna, facing each other. The ground plane was used to form the image, which simulated the existence of the antenna in the “other” wing. We show the complete measurements including the pattern on the back side of the ground plane, for completeness. However, in an operational scenario, the robot would have two antennas facing each other on opposing wings. In this case, the expected pattern can be inferred from our measurements by using the patterns in the upper-half plane only, and reflecting those into the lower-half plane. The resulting pattern was more like a dipole, and was what we would expect to achieve in an operational scenario.

The measured results showed good agreement with the simulated results. As expected, monopole-like radiation patterns having a null in the broadside direction ( $\theta = 0$ ) and an omnidirectional shape in the azimuthal plane were observed. In addition, the measured patterns verified good polarization purity, and a radiation efficiency of 92%. While the fabricated antenna was tested using a ground plane of dimensions 600 mm  $\times$  600 mm, the actual antenna topology for the flapping robotic platform was a dipole version, incorporating the same antenna pattern on the opposite wing. The change in the input impedance from 50 ohms to 100 ohms, resulting from the conversion of the monopole version to the dipole version, could be handled by using a balun with a 100-ohm output impedance.

## 5. Conclusions

This paper demonstrated a method of preparing ultralightweight, high-strength polyimide nanopaper that can be used in applications such as electronic packaging and as a substrate for electronic circuits. As an application of the nanopaper, two conformal antennas on the wings of a flapping robotic platform were presented. The first antenna design used metallic thread formed into a spiral dipole and sandwiched between nanopaper/fiberglass layers. This process was simple and did not require a clean room, but demonstrated a need for careful control of the wire geometry.

The second antenna design required a shadow mask and sputtering system, printing a metallic antenna directly onto the nanopaper. This provided for complex geometrical designs without damaging the nanopaper. The miniaturized folded dipole topology provided reliable impedance matching to a 50-ohm feed.

The design and fabrication techniques presented here can be used in a variety of situations where antennas need to be embedded in low-weight, fabric-like substrates.

## 6. References

1. Jayant Ratti and George Vachtsevanos, “High Endurance, Micro Aerial Surveillance and Reconnaissance Robot,” IEEE Conference on Technologies for Practical Robot Applications (TePRA), Boston, MA, USA, April 2011.
2. Robert C. Michelson, “MicroFlyers and Aerial Robots: Missions and Design Criteria,” RTO AVT Course on “Development and Operation of UAVs for Military and Civil Applications,” Belgium, September 1999.
3. Valerie Woolard, “Reconnaissance Robot Inspired By Natural Designs,” *The Daily Californian*, Sunday, April 20 2008.
4. Daniel W. Beekman, Joseph N. Mait, and Thomas L. Doligalski, “Micro Autonomous Systems and Technology at the Army Research Laboratory,” Proceedings of the IEEE National Aerospace and Electronics Conference (NAECON), OH, USA, July 2008, pp. 159-162.
5. Joseph N. Mait, “The Army Research Laboratory’s Program on Micro-Autonomous Systems and Technology,” Proceedings of SPIE 7318, Micro- and Nanotechnology Sensors, Systems, and Applications, 73180K, May 11 2009.
6. Ahmet Cemal Durgun and Constantine A. Balanis, “Design, Simulation, Fabrication and Testing of Flexible Bow-Tie Antennas,” *IEEE Transactions on Antennas and Propagation*, **AP-54**, 12, December 2011, pp. 4425-4435.
7. S. H. Choi, T.J. Jung, and S. Lim, “Flexible Antenna Based on Composite Right/Left-Handed Transmission Line,” *Electronics Letters*, **46**, 17, August 19 2010, pp. 1181-1182.
8. Haider R. Khaleel, Hussain M. Al-Rizzo, Daniel G. Rucker and Seshadri Mohan, “A Compact Polyimide-Based UWB Antenna for Flexible Electronics,” *IEEE Antennas and Wireless Propagation Letters*, **11**, May 2012, pp. 564-567.
9. S. Kim, Y.-J. Ren, H. Lee, A. Rida, S. Nikolaou and M. M. Tentzeris, “Monopole Antenna With Inkjet-Printed EBG Array on Paper Substrate for Wearable Applications,” *IEEE Antennas and Wireless Propagation Letters*, **11**, June 2012, pp. 663-666.
10. Jungsuek Oh, Kyusang Lee, Tyler W. Hughes, Stephen R. Forrest and Kamal Sarabandi, “Flexible Antenna Integrated with Epitaxial Lift-off Solar Cell Array for Flapping-Wing Robots,” *IEEE Transactions on Antennas and Propagation*, submitted 2012.
11. Robert J. Wood, “Liftoff of a 60mg Flapping-Wing MAV,” Proceedings of the 2007 IEEE/RSJ International Conference on Intelligent Robots and Systems, San Diego, CA, USA, October 2007.

12. Anthony Colazza, "Fly Like a Bird," *IEEE Spectrum*, **44**, 5, 2007, pp. 38-43.
13. Paul Marks, "Bat Drone Shape-Shifts its Wings to Help it Fly," *New Scientist*, **214**, 2866, May 26, 2012.
14. Shivalingappa Lingaiah, Kunigal N. Shivakumar, and Robert Sadler, "Electrospun Nanopaper and its Applications to Microsystems," Proceedings of the International Conference on Composites for the 21st Century – Current and Future Trends, Bangalore, India, January 2011.
15. Marielle Henriksson, Lars A. Berglund, Per Isaksson, Tom Lindström, and Takashi Nishino, "Cellulose Nanopaper Structures of High Toughness," *Biomacromolecules*, **9**, 6, 2007, pp. 1579-1585.
16. Shinichiro Iwamoto, Antonio Norio Nakagaito, Hiroyuki Yano, and Masaya Nogi, "Optically Transparent Composites Reinforced with Plant Fiber-Based Nanofibers," *Applied Physics A: Materials Science and Processing*, **81**, 6, 2005, pp. 1109-1112.
17. Antonio Norio Nakagaito and Hiroyuki Yano, "Novel High-Strength Biocomposites Based on Microfibrillated Cellulose Having Nano-Order-Unit Web-Like Network Structure," *Applied Physics A: Materials Science and Processing*, **80**, 1, 2005, pp. 155-159.
18. Masaya Nogi, Shinichiro Iwamoto, Antonio Norio Nakagaito, and Hiroyuki Yano, "Optically Transparent Nanofiber Paper," *Advanced Materials*, **21**, 2009, pp. 1595-1598.
19. Houssinen Sehaqui, Andong Liu, Qi Zhou, and Lars A. Berglund, "Fast Preparation Procedure for Large, Flat Cellulose and Cellulose/Inorganic Nanopaper Structures," *Biomacromolecules*, **11**, 9, 2010, pp. 2195-2198.
20. Anton Formhals, "Method and Apparatus for Spinning," US Patent 2160962, 1939.
21. Kunigal N. Shivakumar and Shivalingappa Lingaiah, "Ultra Lightweight Materials for Bio-inspired Microsystems," Proceedings of 16th International Conference on Composite Materials, Japan Society of Composite Materials, Tokyo, July 2007.
22. Shivalingappa Lingaiah, Kunigal N. Shivakumar, and Robert Sadler, "Electrospinning of Nylon-66 Polymer Nanofabrics," Proceedings of 49th AIAA/ASME/ASCE/AHS/ASC Structural Dynamics and Materials Conference, Schaumburg, IL, April 2008.
23. Shivalingappa Lingaiah and Kunigal N. Shivakumar, "Electrospun High Temperature Polyimide Nanopaper," *European Polymer Journal*, **49**, 8, 2013, pp. 2101-2108.
24. A. Nathan, A. Ahnood, M. T. Cole, Sungsik Lee, Y. Suzuki, P. Hiralal, F. Bonaccorso, T. Hasan, L. Garcia-Gancedo, A. Dyadyusha, S. Haque, P. Andrew, S. Hofmann, J. Moultrie, Daping Chu, A. J. Flewitt, A. C. Ferrari, M. J. Kelly, J. Robertson, G. A. J. Amaratunga, and W. I. Milne, "Flexible Electronics: The Next Ubiquitous Platform," *Proceedings of the IEEE*, **100**, 5, 2012, pp. 1486-1517.
25. Chin-Chin Tsai, "Recent Development in Flexible Electronics," Optoelectronics and Communications Conference (OECC), 2011, pp. 370-371.
26. Seiichi Takamatsu, Takahiko Imai, Takahiro Yamashita, Takeshi Kobayashi, Koji Miyake, and Toshihiro Itoh, "Flexible Fabric Keyboard with Conductive Polymer-Coated Fibers," IEEE Sensors Conference, October 2011, pp. 659-662.

## Introducing the Feature Article Authors



**Kamal Sarabandi** received the BS in EE from Sharif University of Technology in 1980. He received the MS in EE (1986), the MS in Mathematics, the PhD in Electrical Engineering from the University of Michigan, Ann Arbor, in 1989. He is the Rufus S. Teesdale Professor of Engineering and Director of the Radiation Laboratory in the Department of Electrical Engineering and Computer Science at the University of Michigan. His research areas of interest include microwave and millimeter-wave radar remote sensing, metamaterials, electromagnetic wave propagation, and antenna miniaturization.

He has 22 years of experience with wave propagation in random media, communication-channel modeling, microwave sensors, and radar systems. He leads a large research group, including two research scientists, 12 PhD and two MS students. He has graduated 31 PhDs and supervised numerous postdoctoral students. He has served as the principal investigator on many projects sponsored by NASA, JPL, ARO, ONR, ARL, NSF, DARPA, and a larger number of industries. Dr. Sarabandi has published many book chapters and more than 170 papers in refereed journals on miniaturized and on-chip antennas, metamaterials, electromagnetic scattering, wireless channel modeling, random media modeling, microwave measurement techniques, radar calibration, inverse scattering problems, and microwave sensors. He has also had more than

420 papers and invited presentations in many national and international conferences and symposia on similar subjects.

Dr. Sarabandi is a member of the NASA Advisory Council appointed by the NASA Administrator. He also served as a Vice President of the IEEE Geoscience and Remote Sensing Society (GRSS), and a member of the IEEE Technical Activities Board Awards Committee. He serves on the Editorial Board of the *IEEE Proceedings*, and served as an Associate Editor of the *IEEE Transactions on Antennas and Propagation* and the *IEEE Sensors Journal*. Prof. Sarabandi is a member of Commissions F and D of USNC-URSI, and is listed in *American Men & Women of Science Who's Who in America* and *Who's Who in Science and Engineering*. Dr. Sarabandi was the recipient of the Henry Russel Award from the Regents of the University of Michigan. In 1999, he received a GAAC Distinguished Lecturer Award from the German Federal Ministry for Education, Science, and Technology. He was also a recipient of the 1996 EECS Department Teaching Excellence Award, and a 2004 College of Engineering Research Excellence Award. In 2005, he received the IEEE GRSS Distinguished Achievement Award and the University of Michigan Faculty Recognition Award. He received the Best Paper Award at the 2006 Army Science Conference. In 2008, he was awarded a Humboldt Research Award from the Alexander von Humboldt Foundation of Germany. In the past several years, joint papers presented by his students at a number of international symposia (IEEE AP-S '95, '97, '00, '01, '03, '05, '06, '07; IEEE IGARSS '99, '02, '07; IEEE IMS '01; USNC-URSI '04, '05, '06; AMTA '06; URSI GA 2008) have received student paper awards.



**Jungsoek Oh** received the BS and MS from Seoul National University, Korea, in 2002 and 2007, respectively, and the PhD from the University of Michigan at Ann Arbor in 2012. From 2007 to 2008, he was with Korea Telecom as a hardware research engineer working on the development of flexible RF devices. In 2012, he was a Postdoctoral Research Fellow with the Radiation Laboratory at the University of Michigan. He is currently a Senior RF Engineer with Samsung Research America, Dallas. His research areas include millimeter-wave beam-focusing/shaping techniques, antenna miniaturization for integrated systems, and radio propagation modeling for indoor scenarios. He is the recipient of the 2011 Rackham Predoctoral Fellowship Award at the University of Michigan.



**Leland E. Pierce** received the BS in both Electrical and Aerospace Engineering in 1983, and the MS and PhD in Electrical Engineering in 1986 and 1991, respectively, all from the University of Michigan, Ann Arbor. Since then, he has been the head of the Microwave Image Processing Facility within the Radiation Laboratory in the Electrical Engineering and Computer Science Department at the University of Michigan, Ann Arbor. He is responsible for research into the uses of polarimetric SAR systems for remote sensing applications, especially forest canopy parameter inversion.



**Kunigal Shivakumar** is the Director of the Center for Composite Materials Research and the NASA-funded Center for Aviation Safety at North Carolina Agricultural and Technical State University. He received the BE from Bangalore University, and the ME and PhD from the Indian Institute of Science, India. His research and technical activities include polymer-based composite materials, structural and fracture mechanics, and novel concepts for fire, blast, and damage mitigation. Dr. Shivakumar has engaged in research with NASA, ONR, ARMY, AFRL, NSF, and FAA and major aerospace industries. Dr. Shivakumar has collaborated and is collaborating with a number of universities, including the University of Maryland (College Park), the University of Mississippi, the University of Utah, UC Berkley, and Harvard. He has graduated more than thirty-five PhD and MS students at NCA&T and other universities. Dr. Shivakumar has served in government, industry, and universities. Dr. Shivakumar is an Associate Fellow of AIAA, a member of ASME and ASC, and has been involved in a number of national and international conferences and workshops. He has served in a number of technical committees and societies, specifically in advancing material modeling, testing, and applications. Dr. Shivakumar was an Associate Editor of the *AIAA Journal* and a member of

the Board of Editors of *Computer Modeling and Engineering Sciences*. He was a reviewer for a number of journals in structures and materials. Dr. Shivakumar has published over 200 peer-reviewed articles and made an equal number of presentations in national and international conferences, universities, and companies. He has received many awards from NASA, AIAA, AS&M Inc., North Carolina A&T State University, and the Indian Institute of Science. Dr. Shivakumar is currently associated with a number of faculty, staff, and graduate students from the College of Engineering and College of Arts & Science.

**Shivalingappa Lingaiah** is currently a Senior Research Scientist at the Center for Composite Materials Research in the Department of Mechanical Engineering at the North Carolina Agricultural and Technical State University. He obtained his MSc in Physics and Post Graduate Diploma in Instrumentation from Bangalore University, and his MSc (Eng) and PhD in the Department of Instrumentation from the Indian Institute of Science, India. His research and technical activities include development of electro-spinning systems, preparation and characterization of different polymers for different applications, plasma etching, and three-dimensional visualization of nano-inorganic filler in nanocomposites. He is also involved in the design and development of many new instruments and techniques that are useful in vacuum and thin-film process control. Dr. Lingaiah has graduated six MTech, four MSc (Eng.) students and one PhD student at the Indian Institute of Science and other universities. Dr. Lingaiah has served in government, industry, and universities. Dr. Lingaiah is a Life Member of the Instrument Society of India, Alumini Society of India, and a member of AIAA. Dr. Lingaiah is a reviewer for the *Journal of Instrument Society of India* and the *IEEE Transactions on Industry Applications*. Dr. Lingaiah has more than 80 publications in peer-reviewed journals, conference proceedings, and symposia, and a similar number of presentations in national and international conferences, universities, and companies. He has received many awards, including those from the Japanese Scientific Promotion of Sciences, Japan; Commonwealth Scientific, UK; Indian Institute of Science; Visiting Scientist Fellowship, UK. Dr. Lingaiah's teaching background includes courses on "Thin Film Deposition and Characterization," "Transducers and Measurement Techniques," "Thin Film Devices and Applications," and "Microprocessor-Based Instrumentation." 